Transient interactions studied by NMR : iron sulfur proteins and their interaction partners

Xu, X.

Ferredoxin/ferredoxin-thioredoxin Reductase Complex: Complete NMR Mapping of the Interaction Site on Ferredoxin by Gallium Substitution

Xu X, Kim SK, Schürmann P, Hirasawa M, Tripathy JN, Smith J, Knaff DB, Ubbink M. *FEBS Letters*, 2006, 580, 6714-6720.

Abstract:

The reduction of ferredoxin-thioredoxin reductase by plant-type ferredoxin plays an important role in redox regulation in plants and cyanobacteria. Nuclear magnetic resonance (NMR) was used to map the binding sites on *Synechocystis* ferredoxin for FTR. A gallium-substituted structural analogue of this 2Fe-2S ferredoxin was obtained by reconstituting the apoprotein in a refolding buffer containing gallium. For the first time, the complete interaction interface of a 2Fe-2S ferredoxin with a target enzyme has been mapped by NMR chemical shift perturbation with this diamagnetic structural analogue.

Introduction

Transient complexes formed by electron transfer proteins play an important role in photosynthesis and respiration. One of the most important electron transfer proteins in oxygenic photosynthesis is the soluble 2Fe-2S cluster-containing protein, ferredoxin. This protein, also known as plant-type ferredoxin, is a small (M_r = 11 kDa), acidic (pI = ca. 3) protein [(1)]. It transfers electrons from photosystem I to a range of other proteins including ferredoxin-$NADP^+$ reductase (FNR), ferredoxin-thioredoxin reductase (FTR), glutamate synthase (GOGAT), nitrite reductase (NiR), cyanobacterial nitrate reductase (NaR), sulfite reductase (SiR), and ferredoxin-plastoquinone reductase [(2)].

Most thioredoxin reductases are flavoproteins and use NADPH as reductant. In contrast, FTR is a unique 4Fe-4S enzyme and composed of a conserved catalytic subunit of 13 kDa, with a 4Fe-4S cluster and a proximal redox active disulfide, and a variable subunit of similar size [(3)]. In chloroplasts, FTR receives electrons from Fd and then reduces the thioredoxins *f* and *m* through a disulfide-dithiol interchange system. Thioredoxins can reduce regulatory disulfides of various target enzymes to activate or deactivate them, thus switching on anabolic pathways and inhibiting catabolic ones [(3,4,5)].

Spinach Fd and FTR were shown, using changes in absorbance and circular dichroism difference spectra, to form a 1:1 complex at low ionic strength that dissociates at high ionic strength [(6)]. The K_d of this complex at 15 mM ionic strength is smaller than 10^{-7} M, a value considerably lower than those measured for complexes of ferredoxin with other interaction partners [(6)]. Differential chemical modification of acidic residues of Fd identified D34, D65, E92, E93, E94 and C-terminal A97 as important residues for the binding to FTR [(7)]. Nuclear magnetic resonance can be used to study these complexes in solution, providing detailed information on the interaction interface, and the dynamics of binding [(8,9)]. However, for proteins containing a 2Fe-2S cluster, there is a

challenging problem. Fast relaxation of the nuclear spins located close to the iron sulfur results in NMR signals that are broad or even invisible, so that no information can be obtained for an important area on the protein surface. An obvious way of circumventing paramagnetic broadening is to substitute the iron sulfur center with a diamagnetic prosthetic group.

Here, we use NMR to study the interaction of Fd and FTR, both from *Synechocystis* sp. PCC6803. Replacement of the 2Fe-2S cluster with a gallium ion produces a diamagnetic analogue of Fd that eliminates this problem. Using chemical shift perturbation analysis, the entire binding interface of the complex in solution can be mapped. The results show that the FeS clusters of two proteins are in close proximity in the Fd/FTR complex.

Materials and methods

Protein preparation

A culture of *Escherichia coli* harboring the plasmid containing the Fd gene from *Synechocystis* sp. PCC 6803 [(10)] was grown in LB medium containing ampicillin (100 μg/mL) and 0.5 g ^{15}N ammonium chloride (Cambridge Isotopes Laboratories, Inc., Andover, MA) per L of culture. Fd was expressed in *E. coli* and purified as described previously [(11)] . The ferredoxin concentration was estimated from the absorbance at 422 nm, using an extinction coefficient of 9.8 $mM^{-1}cm^{-1}$. Recombinant FTR from *Synechocystis* PCC6803, produced in *E. coli*, was isolated and purified to homogeneity as described earlier [(12)].

Ga substitution

A solution of the ferredoxin (7 mg/ml in 100 mM Tris-HCl, pH 8.0) was prepared and concentrated HCl was added to the final concentration 1 M. The cloudy solution was centrifuged for 10 min at 14000 rpm. The white precipitate

was immediately rinsed with MilliQ water and re-suspended in degassed 100 mM Tris buffer (pH 8.0). The same procedure was repeated for 3 times to completely remove the FeIII and sulfide. The final protein precipitate was re-suspended in 6 M Gdn.HCl, 100 mM Tris buffer (pH 8.0) containing 10 mM DTT. The apoprotein was refolded at 4 °C by rapid dilution into the refolding buffer containing 2 mM $GaCl_3$, 2 mM Na_2S, 2 mM DTT and 20 mM Tris (pH 8.0). The clear solution was incubated at 4°C overnight. Protein refolding was confirmed by a one-dimensional NMR experiment. Then the protein was applied to a Q-sepharose column, eluted with a gradient of 0 to 1 M NaCl in 20 mM Tris pH 8.0. The protein fractions eluted at 0.5 M NaCl were concentrated by ultrafiltration. The buffer was changed to 20 mM sodium phosphate, pH 7.4 for storage. The concentration of GaFd was determined by the absorbance at 277 nm, using a predicted extinction coefficient of 9.0 $mM^{-1}cm^{-1}$ calculated from the number of tyrosine, tryptophan and cysteine residues [(13)]. A diluted and pure GaFd sample (6.7 µM) in MilliQ water was prepared for gallium element analysis with an Inductively Coupled Plasma (ICP) Optical Emission Spectrometer (Vista-MPX, Varian).

Backbone assignment of native and Ga substituted ferredoxin

NMR samples containing 20 mM sodium phosphate, pH 6.5, 10% D_2O with protein concentration ranging from 0.6 mM to 2 mM for assignment experiments. All NMR experiments were recorded at 293 K on a Bruker DMX600 spectrometer equipped with a TXI-Z-GRAD probe or TXI-Z-GRAD ATM cryo-probe. For sequence-specific assignment of backbone amide resonances of 2Fe-2S Fd and GaFd, 2D heteronuclear ^{1}H-^{15}N-HSQC, 3D ^{15}N-NOESY-HSQC (mixing time 100 ms) and ^{15}N-TOCSY-HSQC (mixing time 60 ms) spectra were recorded. For ^{15}N labeled 2Fe-2S Fd bound to FTR, backbone resonance assignment was performed by the analysis of the sequential NOEs from a 3D ^{15}N-NOESY-HSQC (mixing time 150 ms) for a sample containing

15N Fd:FTR (1.0 mM :1.2 mM). Data were processed with AZARA (http://www.bio.cam.ac.uk/azara/) and resonance assignment was performed in ANSIG-for-Windows [14]

NMR titration and chemical shift mapping

For 2Fe-2S Fd, both normal and reverse titration experiments were performed and followed by recording on ^{1}H-^{15}N HSQC spectra. In the normal titration, 200 μM ^{15}N Fd was titrated with aliquots of 4 mM FTR to a molar ratio of 1.2. In the reverse titration, 200 μM FTR was titrated with aliquots from 2 mM ^{15}N labeled Fd to a molar ratio of 2.8. For GaFd, 90 μM ^{15}N labeled Fd was titrated with aliquots of 2.4 mM FTR to a molar ratio of 1.2. The averaged chemical shift change ($\Delta\delta_{avg}$) of ^{15}N and ^{1}H was calculated with the equation:

$$\Delta\delta_{avg} = \sqrt{\Delta\delta N^2 / 50 + \Delta\delta H^2 / 2} \qquad (4.1)$$

in which $\Delta\delta N$ and $\Delta\delta H$ represent the chemical shift change of the amide nitrogen and proton, respectively.

Results

Ga substitution of Fd

The Ga-substituted plant type ferredoxin was obtained through refolding the apoprotein in a refolding buffer containing excess Ga(III). During the apoprotein preparation, the iron sulfur cluster was completed removed by addition of HCl. Refolding was monitored by one-dimensional proton NMR experiment, showing a good dispersion of chemical shifts of amide protons and methyl groups. Ion exchange chromatography was used to purify the folded protein from the refolding mixture. The yield of folded protein is 20-30%. Gallium element

analysis by ICP-OES indicates that the GaFd contains 1.15 ±0.20 mole of gallium per mole of protein.

Backbone chemical shift assignment of ferredoxin and GaFd

The assignment of the backbone ^{1}H and ^{15}N resonances of 2Fe-2S Fd was performed using 3D ^{15}N -NOESY-HSQC and TOCSY-HSQC spectra and greatly facilitated by the availability of assignments from the literature [15]. Residues 36-48, 61-63, 75-79 were not assigned due to the strong paramagnetic effect of the iron-sulfur cluster. After substitution of the paramagnetic FeS cluster with gallium the complete backbone assignment could be obtained.

The comparison of 2D ^{1}H-^{15}N HSQC spectra of 2Fe-2S Fd and GaFd (Figure 4.1) shows that for most of the observable residues of 2Fe-2S Fd the corresponding resonances of Ga Fd match very well. This indicates that the secondary structure and the fold of the protein are maintained. The conclusion is also supported by the similarities in the sequential NOE connectivity between both forms. Many new resonances are also observed in the spectrum of GaFd, originating from residues located in the vicinity of the metal. In native Fd, these residues are invisible due to the paramagnetic relaxation effects of the 2Fe-2S cluster.

Titration experiments

^{1}H-^{15}N HSQC titration experiments were performed by titrating FTR into ^{15}N labeled 2Fe-2S Fd (normal titration) and ^{15}N Fd into FTR (reverse titration). Both show that the interaction is in the intermediate-slow exchange regime. The off rate (k_{off}) can be estimated to be in the range of 50-100 s^{-1} based on the appearance of several resonances exhibiting small chemical shift perturbations. For residues with large perturbations, two sets of resonances representing free and bound states are visible with

intensities proportional to their fractions (Figure 4.2A). The titration results suggest a 1:1 stoichiometry for the complex of Fd with FTR, consistent with earlier estimates for the complex between these two *Synechocystis* proteins based on spectral perturbation experiments [(12)].

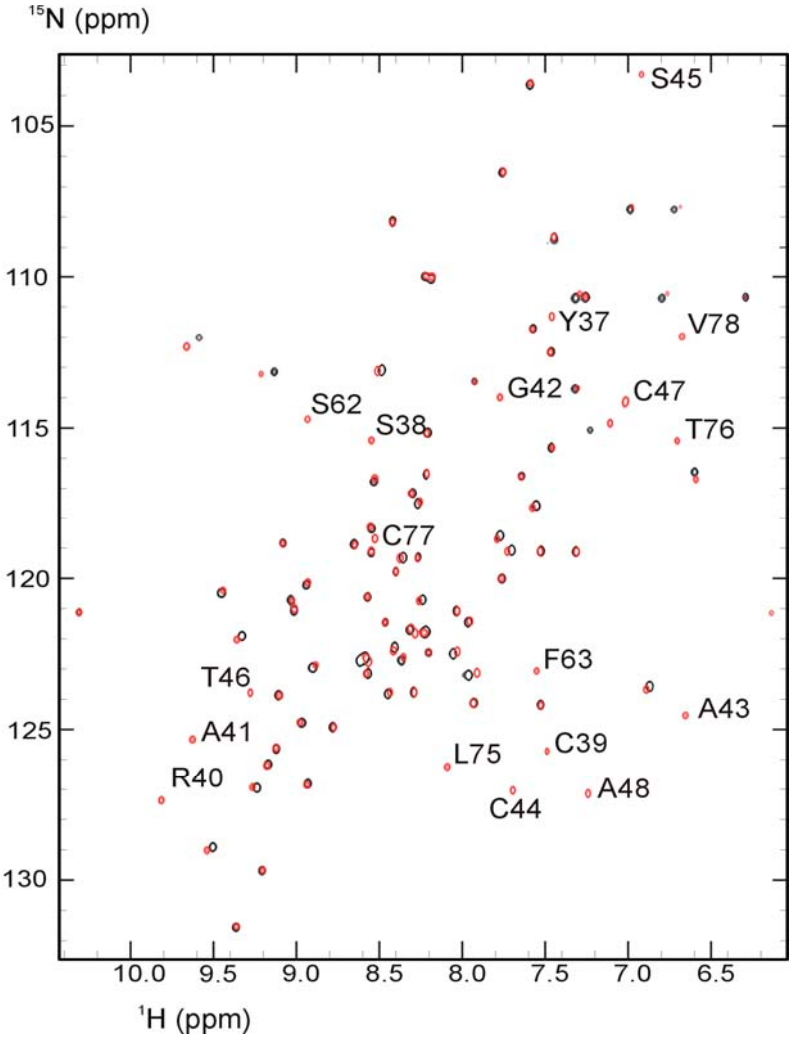

Figure 4.1. Overlay of the HSQC spectra of native Fd (black) and GaFd (red). Assignments of new crosspeaks in the GaFd are indicated with residue numbers.

A titration experiment of FTR into ^{15}N GaFd indicates that the interaction is in the intermediate-fast exchange regime in this case, because the averaged chemical shifts of protein in free and bound states were detected for most of the residues (Figure 4.2B), The assignment of GaFd in bound state was readily achieved by following the chemical shift changes of resonances during titrations. The off rate (k_{off}) can be estimated to be 500 s^{-1} from the resonance of Y96, which is in the intermediate exchange regime because of its large chemical shift difference between free and bound states. At a ratio 1.2 of FTR/GaFd, the chemical shift changes were complete and the chemical shift at this ratio was taken to represent the bound state of Fd.

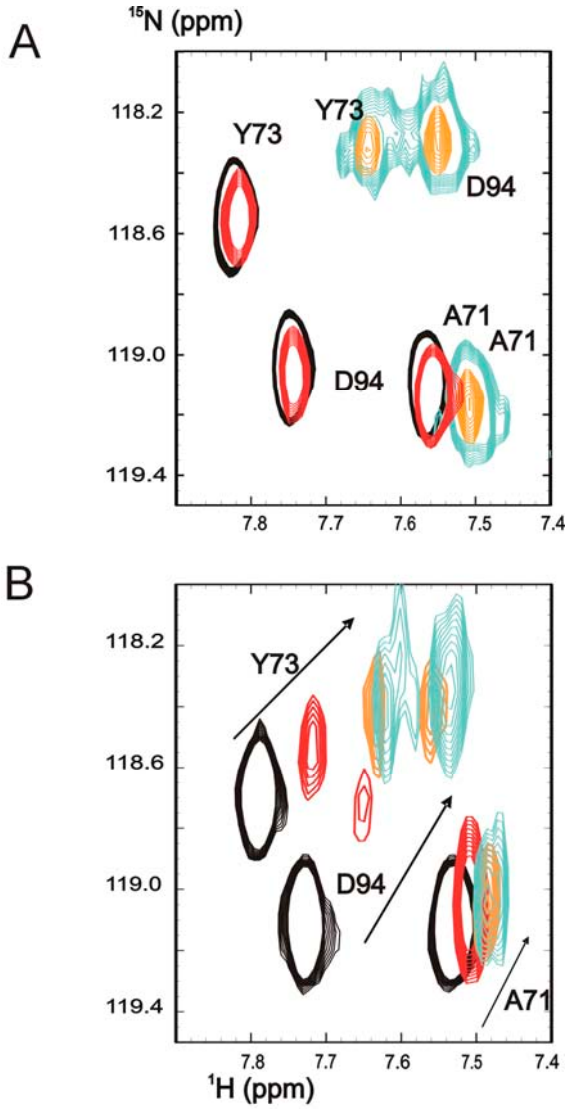

Figure 4.2. Overlay of part of the series of ^{1}H-^{15}N HSQC spectra of the normal titration experiments for 2Fe-2S Fd (A) and GaFd (B) with FTR. For native Fd (A), the ratios of FTR/Fd are 0 (black), 0.3 (red), 0.7 (orange), 1.2 (blue). For ^{15}N GaFd (B), the ratios of FTR/Fd are 0 (black), 0.4 (red), 0.7 (orange), 1.2 (blue)

Intermolecular paramagnetic effect

For residues C39 and R40 in GaFd, the resonances are broadened to a much larger extent than is the case for the rest of the residues, even at a FTR/Fd ratio as low as 0.11 (the first point in the titration). The crosspeaks of these two residues have completely disappeared in the following titration points and do not reappear in the fully bound state. The line broadening of the averaged peaks in fast exchange is proportional to the square of chemical shift difference between the free and the bound states. The large broadening of C39 and R40 cannot be due to this exchange, because the extrapolated chemical shift changes for these two residues are much smaller than the largest observed chemical shift change of residue C44, which is visible in the HSQC spectrum of the last titration point. Thus, we attribute the extra line broadening of C39 and R40 to an intermolecular paramagnetic effect that originates from the paramagnetic Fe-4S iron-sulfur cluster of FTR.

Interaction maps on Fd and GaFd with FTR

Upon binding to FTR, GaFd exhibits similar chemical shift changes in both ^{15}N and proton dimensions compared to observable residues of native Fd (Figure 4.3), suggesting that both forms of ferredoxin use the same residues to interact with FTR. Thus, gallium substitution only changes the kinetics and the affinity of the interaction but not the binding site. In Figure 4.4, the chemical shift changes were mapped onto the residues of crystal structure of Fd (PDB ID:1OFF) [16]. For 2Fe-2S Fd, chemical shift mapping clearly shows that C-terminal residues E92-Y96 and acidic

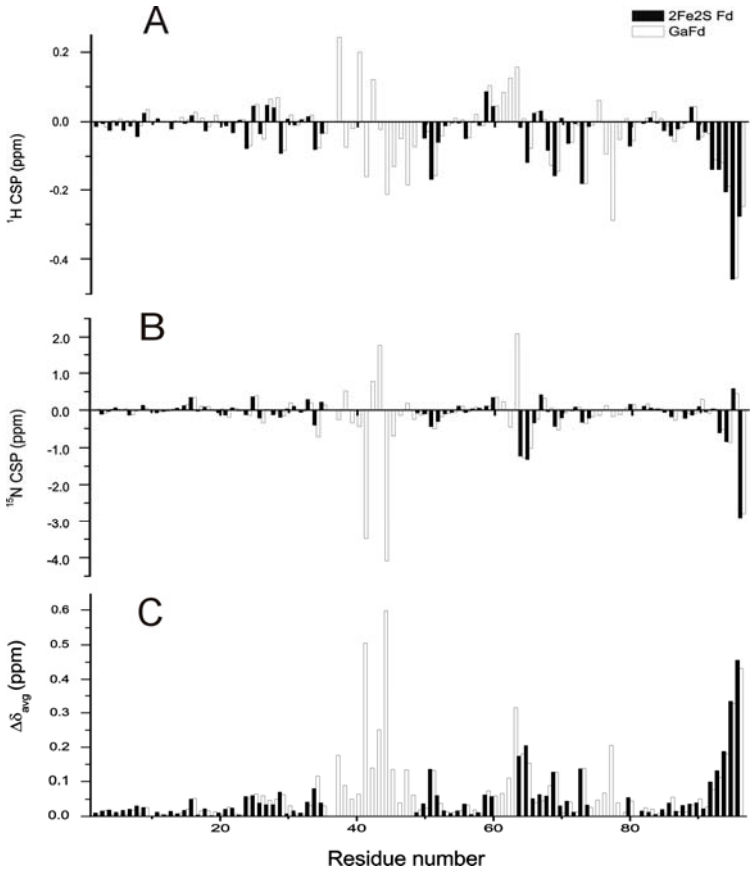

Figure 4.3. Comparison of chemical shift perturbations for native Fd and GaFd upon complex formatin with FTR. Chemical shift changes of amide proton (A), amide nitrogen (B) and $\Delta\delta_{avg}$ (C) of 2Fe-2S Fd (black bars) and GaFd (white bars) are shown for all observed residues

residues D34, D65 are involved in the binding. All these residues display relatively large chemical shift perturbations. However, no information could be obtained for other important residues located close to the iron sulfur cluster (Figure 4.4A). For the GaFd, all residues with large

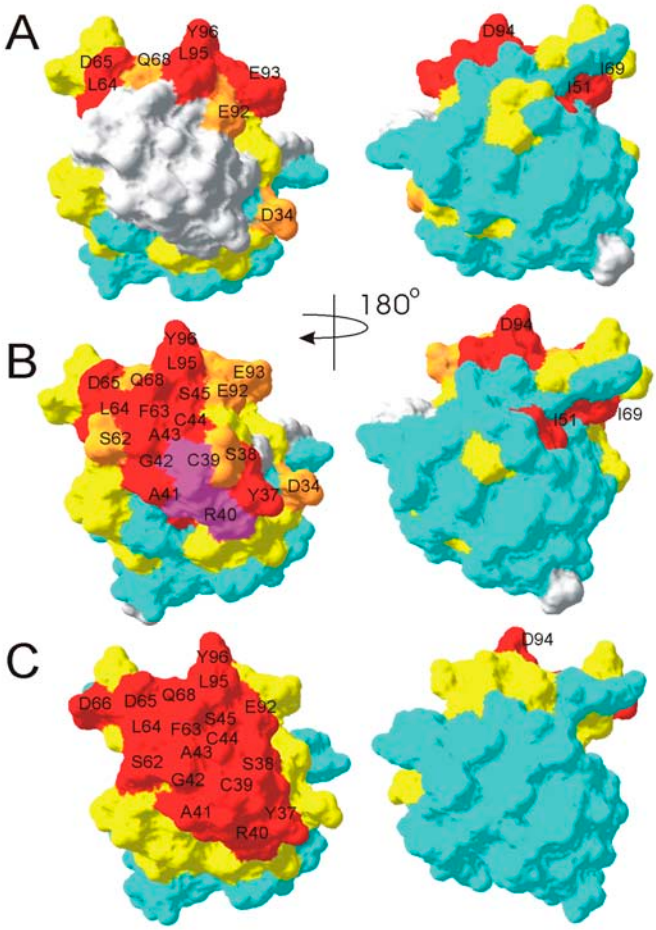

Figure 4.4. Chemical shift mapping on 2Fe-2S Fd and GaFd in the presence of FTR. The crystal structure of *Synechocystis* Fd was used to display the surface generated by Deep-Viewer. Residues are color coded according to $\Delta\delta_{avg}$ (red for ≥ 0.12; orange for ≥ 0.08; yellow for ≥ 0.04; blue for < 0.04), unassigned residues are colored in white. In (B), residues C39 and R40, which experience an intermolecular paramagnetic effect in the GaFd/FTR complex, are colored in purple. (C) Surface representation of the interface on Fd in the cystal structure of Fd/FTR complex. Interface residues with atoms < 5 Å from FTR are colored in red. Residues close to the interface, with atoms < 8 Å from FTR, are colored in yellow.

chemical shift perturbations were identified. They mainly map to D34, Y37-S45 (iron sulfur loop), I51, S62-D65, Q68-I69, Y73, and C-terminal residues E92-Y96 (Figure 4.4B).

Discussion

NMR chemical shift perturbation analysis was used to study the interaction of *Synechocystis* 2Fe-2S Fd with FTR. The titration experiment showed that the interaction of Fd with FTR is in the slow to intermediate exchange regime. Chemical shift mapping with native, paramagnetic Fd shows that all of the residues with large chemical shift changes except I51 are located near the 2Fe-2S loop. However, due to the strong paramagnetic broadening effect of the iron-sulfur cluster, 20 residues located in the vicinity are invisible or difficult to assign in HSQC spectra, leading to the loss of important information.

Metal substitution has been extensively used to study the metallo-proteins. For 2Fe-2S ferredoxin, successful replacement of iron sulfur with a single gallium ion or a gallium sulfur cluster was reported previously, using a denaturation and reconstitution method [17,18]. Gallium substituted putidaredoxin has been structurally characterized by NMR and it was found that Ga putidaredoxin has a structural fold similar to that of 2Fe-2S putidaredoxin, even though the iron sulfur loop conformation was slightly distorted by the single gallium substitution [19].

A similar denaturing and refolding method was used in our study to achieve the gallium substitution for plant type 2Fe-2S Fd. NMR spectra indicate that GaFd has a folded structure similar to native Fd. Gallium elemental analysis of the *Synechocystis* GaFd used in this study indicates that one gallium atom was incorporated per protein molecule. Based on the sequence homology of plant-type ferredoxin and of putidaredoxin, it seems reasonable to conclude that Ga is

bound in the *Synechocystis* Fd in a manner similar to that reported for Ga putidaredoxin, resulting in a product in which the gallium coordinates with 4 cysteine sulfurs.

The chemical shift perturbation results suggest that GaFd is a good structural analog of native Fd and thus suitable for mapping the FTR-interaction sites of Fd within the 1:1 Fd/FTR complex. Surprisingly, the interaction of GaFd with FTR is in the intermediate-fast exchange regime. A plausible explanation is that the distortion of loop region (residues P36-S45) introduced by single gallium substitution slightly alters the surface complementarities of Fd and FTR or the charge of Fd, resulting in a reduced affinity and an increase of k_{off}. This phenomenon may offer advantages for the chemical shift mapping of tight large protein complexes formed by Fd with its interaction partners such as Fd/NiR complex, Fd/NaR complex and Fd/GOGAT complex. The fast exchange regime facilitates the resonance assignment of Fd in the bound state by avoiding the need for deuteration of the protein and TROSY experiments [(20)] on the large protein complexes.

With the GaFd, a complete chemical shift map of Fd for the interaction with FTR was obtained. Most of the hydrophobic residues located in or close to the iron-sulfur loop were strongly perturbed by complex formation. It can be concluded that this region is involved in the binding while the amide of residue I51, located on the other side of the protein, probably experiences a secondary chemical shift change resulting from the perturbation of hydrogen bond with G72 upon complex formation. The result of NMR mapping in this study is consistent with the previous mapping by differential chemical modification experiments on spinach Fd and FTR [(7)]. A comparison of our NMR chemical shift mapping to the interface of the Fd/FTR complex observed in the crystal structure ([(21)] and Dai, S. et al, unpublished observations) also confirmed the validity of this diamagnetic analog. In the crystal structure of Fd/FTR complex from *Synechocystis*, Fd residues Y37-T46, Q61-D66, Q68, E92, L95-Y96 are in

the interface while other residues including E29, E34, P36, C47-K50, Q58-D60, D67, I69, H90-K91, D93-D94 are very close to the interface (Figure 4.4C).

The $\Delta\delta_{avg}$ values can be classified as large. Worrall et al [22] have shown that $\Delta\delta_{avg}$ values can vary greatly between protein complexes. This was attributed to the degree of dynamics within the complex. The large $\Delta\delta_{avg}$ values observed here classify the Fd/FTR complex as a well-defined complex, with little internal dynamics.

The intermolecular paramagnetic effect detected on diamagnetic GaFd is an interesting observation. The 4Fe-4S cluster is in the 2+ state in purified FTR, and is EPR silent [23]. However, at room temperature low lying excited states are populated rendering the cluster paramagnetic [24]. Intermolecular paramagnetic effects including pseudo contact shifts and paramagnetic relaxation enhancement can provide useful restraints in modeling of protein-protein interactions, as was shown previously [25]. In this case, the extra broadening effect due to the intermolecular paramagnetic relaxation enhancement may be exploited to determine the orientations of the proteins in the complex in solution.

Plant-type Fd can interact with a number of different redox enzymes. An interesting question is how electron flow is regulated and balanced in this complex interaction network [26]. An increasing number of studies on the interaction of Fd with different enzymes suggests that the differences in the interactions of conserved acidic residues which are distributed in three separate acidic patches on the surface of Fd, may well provide the answer to this question. These three patches include residues E29-D34, residues D65-E70 and residues E92-D94 of Fd in the interaction of *Synechocystis* Fd with FTR. Some residues are important for Fd interaction with many partners, others are specific. Our complete chemical shift mapping reveals that not all the residues in these acidic patches are directly involved in binding. The C-terminal acidic patch seems the most important in the interaction of Fd with FTR, an observation also made based on site-directed mutagenesis studies [27]. In contrast, the acidic

patches formed by D65-D66 and E92-E94 on maize Fd are most important in its interaction with maize FNR [28]. Interestingly, the complex formed between FNR and Fd when both proteins come from the cyanobacterium *Anabaena* sp. PCC7119 shows some significant differences in portions of the interactions domain when compared to the complex between the same two maize proteins [29]. In the case of another higher plant, Fd-dependent enzyme, maize SiR, the major interaction sites on maize Fd with SiR include the acidic patch E29-D34 and the C-terminal patch [30].

The interface shown in Figure 4.4 emphasizes, however, that, in addition to the charged residues, polar and non-polar residues are also very important for the interaction. The interface exhibits a composition typical for an electron transfer complex [8,31] with a hydrophobic core (C39, A41, G42, C44, F63, L64, L95) surrounded by polar residues with the charged groups on the outer ring of the interface.

Reference List

1. Fukuyama K. (2004) Structure and function of plant-type ferredoxins. *Photosynth.Res.* **81**: 289-301.
2. Hase, T, Schürmann, P, and Knaff, D. B 2006. Ferredoxin and ferredoxin-dependent enzymes. In Golbeck J.H, Photosystem I: The light-driven, plastocyanin:ferredoxin oxidoreductase: 333-361. Dordrecht, The Netherlands: Kluwer.
3. Dai S.D., Schwendtmayer C., Schürmann P., Ramaswamy S., and Eklund H. (2000) Redox signaling in chloroplasts: Cleavage of disulfides by an iron-sulfur cluster. *Science* **287**: 655-658.
4. Dai S.D., Johansson K., Miginiac-Maslow M., Schürmann P., and Eklund H. (2004) Structural basis of redox signaling in photosynthesis: structure and function of ferredoxin : thioredoxin reductase and target enzymes. *Photosynth.Res.* **79**: 233-248.
5. Schürmann P. (2003) Redox signaling in the chloroplast: The ferredoxin/thioredoxin system. *Antioxid Redox Sign* **5**: 69-78.
6. Hirasawa M., Droux M., Gray K.A., Boyer J.M., Davis D.J., Buchanan B.B., and Knaff D.B. (1988) Ferredoxin-thioredoxin reductase - properties of its complex with ferredoxin .3. *Biochim.Biophys.Acta* **935**: 1-8.
7. De Pascalis A.R., Schürmann P., and Bosshard H.R. (1994) Comparison of the binding-sites of plant ferredoxin for 2 ferredoxin-dependent enzymes. *FEBS Lett.* **337**: 217-220.
8. Crowley P.B. and Ubbink M. (2003) Close encounters of the transient kind: Protein interactions in the photosynthetic redox chain investigated by NMR spectroscopy. *Acc.Chem.Res.* **36**: 723-730.

9. Ubbink M. (2004) Complexes of photosynthetic redox proteins studied by NMR. *Photosynth.Res.* **81**: 277-287.
10. Guillouard I., Lagoutte B., Moal G., and Bottin H. (2000) Importance of the region including aspartates 57 and 60 of ferredoxin on the electron transfer complex with photosystem I in the cyanobacterium *Synechocystis* sp PCC 6803. *Biochem.Biophys.Res.Commun.* **271**: 647-653.
11. Schmitz S., Navarro F., Kutzki C.K., Florencio F.J., and Böhme H. (1996) Glutamate 94 of [2Fe-2S]-ferredoxins is important for efficient electron transfer in the 1:1 complex formed with ferredoxin-glutamate synthase (GltS) from *Synechocystis* sp PCC 6803. *BBA-Bioenergetics* **1277**: 135-140.
12. Glauser D.A., Bourquin F., Manieri W., and Schürmann P. (2004) Characterization of ferredoxin : thioredoxin reductase modified by site-directed mutagenesis. *J.Biol.Chem.* **279**: 16662-16669.
13. Pace C.N., Vajdos F., Fee L., Grimsley G., and Gray T. (1995) How to measure and predict the molar absorption-coefficient of a protein. *Protein Sci.* **4**: 2411-2423.
14. Helgstrand M., Kraulis P., Allard P., and Hard T. (2000) Ansig for Windows: An interactive computer program for semiautomatic assignment of protein NMR spectra. *J.Biomol.NMR* **18**: 329-336.
15. Lelong C., Sétif P., Bottin H., André F., and Neumann J.M. (1995) H-1 and N-15 NMR sequential assignment, secondary structure, and tertiary fold of [2Fe-2S] ferredoxin from *Synechocystis* sp PCC6803. *Biochemistry* **34**: 14462-14473.
16. van den Heuvel R.H.H., Svergun D.I., Petoukhov M.V., Coda A., Curti B., Ravasio S., Vanoni M.A., and Mattevi A. (2003) The active conformation of glutamate synthase and its binding to ferredoxin. *J.Mol.Biol.* **330**: 113-128.
17. Kazanis S., Pochapsky T.C., Barnhart T.M., Pennerhahn J.E., Mirza U.A., and Chait B.T. (1995) Conversion of a Fe_2S_2 ferredoxin I into a Ga^{3+} rubredoxin. *J.Am.Chem.Soc.* **117**: 6625-6626.
18. Vo E., Wang H.C., and Germanas J.P. (1997) Preparation and characterization of [2Ga-2S] *Anabaena* 7120 ferredoxin, the first gallium-sulfur cluster-containing protein. *J.Am.Chem.Soc.* **119**: 1934-1940.
19. Pochapsky T.C., Kuti M., and Kazanis S. (1998) The solution structure of a gallium-substituted putidaredoxin mutant: GaPdx C85S. *J.Biomol.NMR* **12**: 407-415.
20. Pervushin K., Riek R., Wider G., and Wüthrich K. (1997) Attenuated T2 relaxation by mutual cancellation of dipole-dipole coupling and chemical shift anisotropy indicates an avenue to NMR structures of very large biological macromolecules in solution. *Proc.Natl.Acad.Sci.U.S.A.* **94**: 12366-12371.
21. Dai, S., Hallberg, K., Schürmann, P., and Eklund, H 2006. Light/dark regulation of chloroplast metabolism. In Wise,R.R. and Hoober,J.K., The Structure and Funtion of Plastids: 221-236. Dordrecht, The Netherlands.: Springer.
22. Worrall J.A.R., Reinle W., Bernhardt R., and Ubbink M. (2003) Transient protein interactions studied by NMR spectroscopy: The case of cytochrome *c* and adrenodoxin. *Biochemistry* **42**: 7068-7076.
23. Staples C.R., Ameyibor E., Fu W.G., Gardet-Salvi L., Stritt-Etter A.L., Schürmann P., Knaff D.B., and Johnson M.K. (1996) The function and properties of the iron-sulfur center in spinach ferredoxin:thioredoxin reductase: A new biological role for iron-sulfur clusters. *Biochemistry* **35**: 11425-11434.
24. I.Bertini and C.Luchinat (1996) NMR of paramagnetic substances. *Coord.Chem.Rev.* **150**: 1-292.
25. Ubbink M., Ejdebäck M., Karlsson B.G., and Bendall D.S. (1998) The structure of the complex of plastocyanin and cytochrome *f*, determined by paramagnetic NMR and restrained rigid-body molecular dynamics. *Structure* **6**: 323-335.
26. Blankenship R.E. (2001) It takes two to tango. *Nat.Struct.Biol.* **8**: 94-95.

27. Jacquot J.P., Stein M., Suzuki K., Liottet S., Sandoz G., and Miginiac-Maslow M. (1997) Residue Glu-91 of *Chlamydononas heinhardtii* ferredoxin is essential for electron transfer to ferredoxin-thioredoxin reductase. *FEBS Lett.* **400**: 293-296.
28. Kurisu G., Kusunoki M., Katoh E., Yamazaki T., Teshima K., Onda Y., Kimata-Ariga Y., and Hase T. (2001) Structure of the electron transfer complex between ferredoxin and ferredoxin-NADP(+) reductase. *Nat.Struct.Biol.* **8**: 117-121.
29. Morales R., Charon M.H., Kachalova G., Serre L., Medina M., Gomez-Moreno C., and Frey M. (2000) A redox-dependent interaction between two electron-transfer partners involved in photosynthesis. *EMBO Rep.* **1**: 271-276.
30. Saitoh T., Ikegami T., Nakayama M., Teshima K., Akutsu H., and Hase T. (2006) NMR study of the electron transfer complex of plant ferredoxin and sulfite reductase - Mapping the interaction sites of ferredoxin. *J.Biol.Chem.* **281**: 10482-10488.
31. Prudencio M. and Ubbink M. (2004) Transient complexes of redox proteins: structural and dynamic details from NMR studies. *J.Mol.Recognit.* **17**: 524-539.